Journal of Visualization, Vol. 10, No. 3 (2007)309-316

Regular Paper

Transition of Free-Surface Flow Modes in Taylor-Couette System

Watanabe, T.*[1], Furukawa, H.*[2] and Toya, Y.*[3]

*1 EcoTopia Science Institute, Nagoya University, Nagoya, 464-8603, Japan.
E-mail: t-watanabe@esi.nagoya-u.ac.jp
*2 Faculty of Science and Technology, Meijo University, Nagoya, 468-8502, Japan.
*3 Faculty of Mechanical Engineering, Nagano National College of Technology, Nagano, 381-8550, Japan.

Received 30 November 2006
Revised 16 April 2007

Abstract : This paper presents our numerical and experimental results of the bifurcation found in Taylor-Couette system with a free surface. The lengths of the two concentric cylinders are finite and their axes are parallel to the direction of the gravitational force. When the end walls of the cylinders are fixed and stationary, numerical and experimental studies have shown that the flow has multiple patterns depending on the cylinder lengths and the Reynolds numbers. Experimental studies on flows with free surfaces also gave various flow modes. Our result shows that the measured and predicted time-dependent displacements of the free surface are in favorable agreement. In case of the cylinder length comparable with the gap width between the cylinders, gradual accelerations of the inner cylinder bring the normal mode flows with one, three and five toroidal vortices. The exchanges of stabilities between these flow modes are summarized in a phase diagram.

Keywords : Bifurcation, Stability, Free surface flow, Gravitational force, Taylor-Couette flow.

1. Introduction

Mode transitions found in Taylor-Couette system with finite cylinder lengths was addressed in terms of low-order bifurcation events (Benjamin, 1978), and their properties have been discussed in detail (Tagg, 1994; Watanabe et al., 2002; Fraňa et al., 2005; Hantao et al., 2006). This system has solid walls on both ends of cylinders and shows a geometrical symmetry with respect the axial direction (symmetric system). In this paper, we consider Taylor-vortex flows with an additional degree of freedom: a free surface. The axes of the cylinders are parallel to the gravitational force, and the free surface appears at the top while the bottom end plate is stationary. This flow system does not hold its symmetry in the axial direction and it is an asymmetric system.

Some studies were conducted on multi-phase flows and free surface flows around a rotating cylinder (e.g., Baier and Graham, 1998; Gelfgat et al., 2004). The concern of these studies was about the influence of density differences whose effect appeared on instabilities of radially separated flows and axially banded flows. However, the gravitational force was assumed to be small and it was ignored. Michalland et al. (1993) and Bellon et al. (1998) considered directional viscous fingering around a rotating cylinder with a horizontal axis. The origin of their studies lay on Hele-Shaw flows and thin share layers, and no interest was on the liquid-gas interface of the rotating flows. Linek and Ahlers (1998) performed their experimental observations of flows in the asymmetric system similar to the one studied in this paper. They investigated the mechanism found during the transition from decelerating Taylor-vortex flows to circular Couette flows.

Special interests in bifurcation of Taylor-vortex flows with a free surface at the top have been found by one of the present authors. He considered interactions between bottom end wall and the free surface and carried out experimental studies to reveal transitions between multiple modes Taylor-vortex flows (Nakamura et al., 1989; Toya et al., 1994; Nakamura and Toya, 1996). We take over these experiments and adopt our new numerical approach, and investigate the transition in the asymmetric system. The result obtained in this study is useful, for example, to establish an optimal control method which runs fluid and chemical machinery more efficiently.

2. Formulation

2.1 Numerical Method

We consider Taylor-Couette system where the two cylinders are concentric and their axes are parallel to the gravitational force (Fig. 1). The outer cylinder is stationary and the inner cylinder rotates, and their radii are r_{out} and r_{in}, respectively. The bottom end wall of the cylinders is a fixed wall and a free surface appears at the top.

Reference values are the length $D = r_{out} - r_{in}$ and the velocity U which is given as the maximum velocity attained during each run of an experiment or a numerical calculation. The reference time is the fraction of the reference length to the reference velocity. The geometric parameters representing the system are the radius ratio of cylinders η and the aspect ratio Γ,

$$\eta = r_{in} / r_{out}, \qquad \Gamma = L / D, \tag{1}$$

where L is the height of the quiescent working fluid between cylinders. The surface tension and the gravitational force are considered, and the parameters governing the flow are the Reynolds number, the Weber number and the Froude number given by

$$Re = UD / \nu, \qquad We = \rho D U^2 / \sigma, \qquad Fr = U / \sqrt{gD}. \tag{2}$$

Here, ν and ρ are the kinematic viscosity and the density of the working fluid, and σ is the surface tension between the working fluid and the air. The gravitational acceleration on the earth is g.

The behavior of the free surface is modeled by the volume of the fluid method. Let F be the volume fraction of the working fluid in the region surrounded by discrete grid lines. The contact angle between the free surface and the solid cylinder wall is the right angle. The equation of continuity, the unsteady axisymmetric Navier-Stokes equations and the conservation equation of F are given by

$$\nabla \cdot \boldsymbol{u} = 0, \tag{3}$$

$$\frac{\partial \boldsymbol{u}}{\partial t} + \nabla \cdot (\boldsymbol{uu}) = -\nabla p + \frac{1}{Re} \nabla^2 \boldsymbol{u} + \frac{\boldsymbol{g}}{Fr^2}, \tag{4}$$

$$\frac{\partial F}{\partial t} + \nabla \cdot (\boldsymbol{u} F) = 0. \tag{5}$$

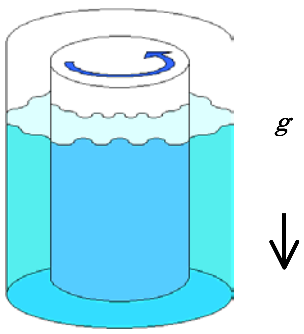

Fig. 1. Free surface flow developing between concentric cylinders. The axes of cylinders are parallel to the direction of the gravitational acceleration. The inner cylinder rotates and the outer cylinder and the bottom end wall are fixed.

They are given in the dimensionless cylindrical coordinate system (r,θ,z) with time t made dimensionless by the reference time, and the axis z is vertical upward. The velocity vector $\boldsymbol{u}$ has its components u, v and w. The pressure is p and the gravitational acceleration vector is $\boldsymbol{g}$.

The surface profile is estimated by the five-point smoothing function. The smoothed surface profile z_s is used to evaluate the effect of the surface tension. The curvature of the surface and the pressure increment by the presence of the curvature are given by

$$\kappa = \frac{\partial^2 z_s / \partial r^2}{(1+(\partial z_s / \partial r)^2)^{3/2}}, \tag{6}$$

$$\Delta p_s = -\frac{\kappa}{We}. \tag{7}$$

In this formulation based on the axisymmetric equations, the only primary curvature we consider is the one in the radial direction, while the curvature in the circumferential direction is assumed to be small and it is omitted (Batchelor, 1967).

The spatial discretization of the governing equations is the finite difference method, and the time integration is the fractional step. The boundary conditions of velocity components are the non-slip conditions on the solid wall, and the boundary condition of the pressure equation is the Neumann condition estimated from the momentum equations.

2.2 Experiment and Conditions

The experimental apparatus has a stainless steel inner cylinder with radius 40 mm and an acrylic outer cylinder with radius 60 mm. The radius ratio η is 0.667, and the dimensionless radii of the inner cylinder and the outer cylinder are 2.0 and 3.0, respectively. In the Taylor-vortex system between finite-length cylinders, the critical Reynolds number for the onset of Taylor vortex is 76.3 at η = 0.667 (Di Prima and Swinney, 1981). A small amount of aluminum flakes was used as an additive for visualization observations, and the behaviors of flows were recorded by a still camera and a video camera.

The working fluid is an aqueous solution of glycerol, and its density, kinematic viscosity and surface tension are 935 kg/m^3, 9.54×10^{-6} m^2/s and 2.07×10^{-2} N/m, respectively. The gravitational acceleration g is 9.8 m/s^2. These property values are adopted to convert experimentally obtained values to numerically predicted values and vice versa.

The behavior of the free surface was measured in the flow at Γ = 5.7. At this aspect ratio, it was confirmed that the effect of the acceleration rate of the inner cylinder on the fully developed flow

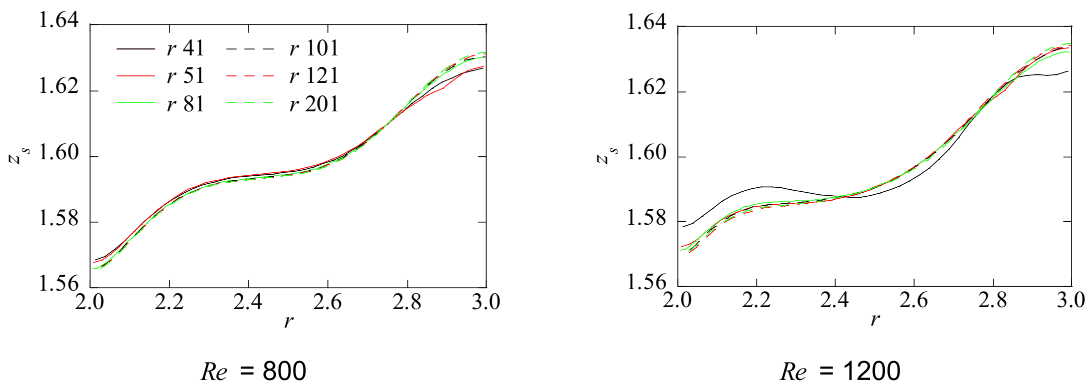

Fig. 2. Grid refinement study. The profiles of the free surfaces at Γ = 1.6 and the dimensionless time t = 1200. The notation *rn* represents that the number of the radial grid points is *n*.

is small and the flow in the five-cell mode appears at high probability. The definition of flow modes found in the symmetric system and the asymmetric system is well summarized by Toya et al. (1994).

In the numerical simulation, the flow at an initial state is stationary, and the circumferential velocity of the inner cylinder is linearly increased to the value which presents a prescribed Reynolds number. The increment in the Reynolds number is 8386 per viscous time scale D^2/ν, which corresponds to the acceleration of 200 per second in the dimensional form. This linear acceleration assures unique flows at given Reynolds numbers and fixed aspect ratios. The numerical study was done at the aspect ratio from 0.8 to 5.0.

The grid interval of the finite difference method is uniform in the radial and the axial directions. The number of the axial grid points is determined by the aspect ratio times a given number of the radial grid points. Numerical results are obtained by using some resolutions to perform a grid refinement study. As an example of this study for the radial grid points of 41, 51, 81, 101, 121 and 201, Fig. 2 shows the displacement of the free surface, which is represented by $z_s(r)$, at Γ = 1.8 and the dimensionless time t = 1200. When the number of the radial grid points is greater than or equal to 81, the profiles are almost identical. From this study, the radial grid points of 101 and 121 are used in the present simulation.

3. Results

3.1 Transient Process of Flow Development

Figure 3 shows the time variation of flow vectors (u, w) in the meridional section of the system at Γ = 1.6, Re = 800. The linear acceleration of the inner cylinder ends at the dimensionless time t = 76.32. In each figure, the inner cylinder is on the left side and the outer cylinder is on the right side, and the free surface is at the top and the stationary end wall is at the bottom.

In the first state at t = 16.0, a vortex appears at the inner and lower corner of the section.

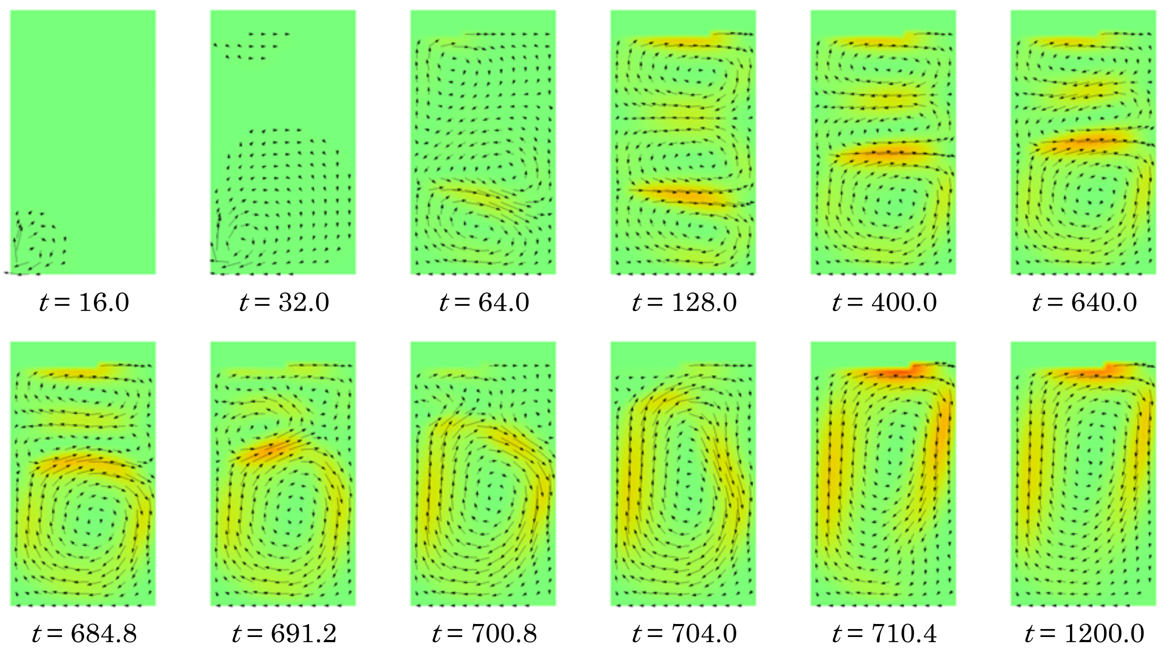

Fig. 3. Time variation of flow vectors (u, w) in the meridional section of the flow at Γ = 1.6, Re = 800. The linear acceleration of the inner cylinder ends at the dimensionless time t = 76.32.

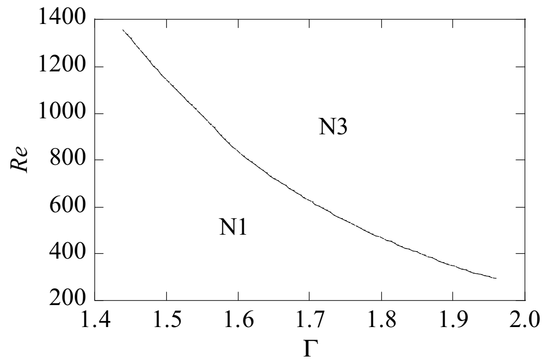

(a) Critical locus between N1 and N3.

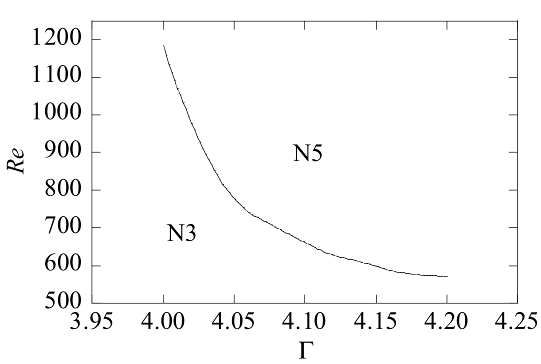

(b) Critical locus between N3 and N5.

Fig. 4. Bifurcation diagrams of the normal one-cell mode (N1), the normal three-cell mode (N3) and the normal five-cell mode (N5) in the asymmetric system with free surface.

Another vortex can be found near the free surface at t = 32.0, and the flow with three vortices is established by t = 128.0.

The asymmetric system has a free surface on the upper side and the usual flow direction there is from the inner cylinder wall to the outer cylinder wall, which means an outward flow. On the other hand, the flow is retarded on the bottom end wall and the flow direction is expected to be inward. These flow directions match our physical intuition, and the modes of flows with these flow directions are defined as the normal modes.

The flow at t = 128.0 is in the normal mode and it has three vortices, the flow mode is called the normal three-cell mode. This flow is not stable and it is gradually deformed. Then the flow pattern changes to the one with one vortices (the normal one-cell mode) in a short duration around t = 690.0 to 710. When the Reynolds number is larger, the flow of the normal three-cell mode remains. As will be seen later, this results in the bifurcation of the normal three-cell mode and the normal one-cell mode. In the figures of developed flows at t = 128.0 and later, the centrifugal force of the rotating flow raises the location of the free surface higher near the outer cylinder.

3.2 Bifurcation of Flows

Bifurcation diagrams in the asymmetric system are shown in Fig. 4. The normal one-cell mode (N1) and the normal three-cell mode (N3) appear at Γ from 1.44 to 1.96, and the primary mode which is defined as a mode appearing at lower Reynolds number is the normal one-cell mode. At Γ from 4.0 to 4.26, the primary mode is the normal three-cell mode, and the normal five-cell mode (N5) emerges at higher Reynolds number. The critical Reynolds number for the exchange of flow modes decreases with the aspect ratio. No mode other than the normal tree-cell mode appears at the aspect ratio larger than 1.96 and less than 4.0.

In order to estimate the effect of the mode exchanges on time variations of the flows, two time dependent variables are used. One is the volume-averaged energy of the axial velocity component w at time t

$$E_w(t) = \frac{1}{Q}\int_Q \frac{w^2}{2} d\boldsymbol{q}, \tag{8}$$

where Q is the three-dimensional annulus region filled by working fluid, and the other is the time-dependent displacement of the free surface at the midpoint radial position between cylinders, which is denoted by $z_m(t)$. Then the time variances of these values

$$\sigma_w^2 = \frac{1}{T}\int_t^{t+T} (E_w(t) - \overline{E_w})^2, \tag{9}$$

$$\sigma_m^2 = \frac{1}{T}\int_t^{t+T} (z_m(t) - \overline{z_m})^2, \tag{10}$$

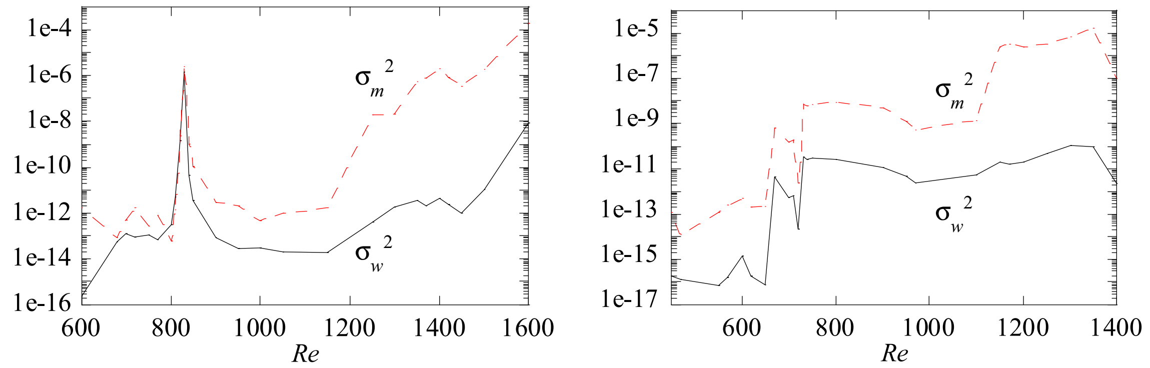

(a) Γ = 1.6. (b) Γ = 4.1.

Fig. 5. Variances of the volume-averaged energy of the axial velocity component and the displacement of the free surface.

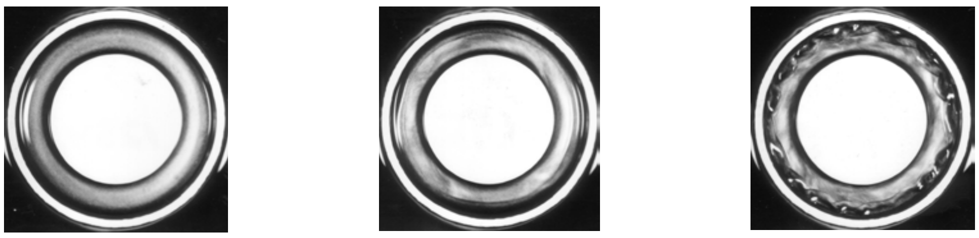

Re = 1259 *Re* = 1595 *Re* = 1877

Fig. 6. Experimental observations of free surface flows in top views. The white circular plane in the center is the inner cylinder rotating in the counterclockwise direction and the surrounding thin rim is the acrylic outer cylinder. Γ = 5.7.

are evaluated. Here, the over bar means the time average and the time integral is performed for fully developed flows. The variations of σ_w^2 and σ_m^2 with the Reynolds number are shown in Fig. 5. The aspect ratios Γ are 1.6 and 4.1, and the critical Reynolds number of the mode exchanges are about 835 and 660, respectively. The values of the variances grow rapidly at these critical Reynolds numbers. Similar growth at the mode changes was found at another aspect ratio. This means that the mode exchanges present temporal instabilities, as well as flow pattern instabilities.

3.3 Experimental Observation of Flows

Figure 6 gives top-view photographs of experimentally observed flows. The inner cylinder rotates in the counterclockwise direction. Two light sources were place at the upper and the lower sides in each photograph. The free surface with a slight gradient includes flat aluminum flakes along it and it appears as a bright region in the flow field, while the surface in the dark region is relatively steep. When the Reynolds number is small, weak distortions of the surface profile appear and circular waves rise. As the Reynolds number increases, the axisymmetic flow ceases and traveling waves with a fixed phase velocity emerge. At *Re* = 1259, the flow keeps its axisymmetry and the waves are weak circular waves. Deformation of the profile around the cylinders remains small at *Re* = 1595, while the traveling waves grows at *Re* = 1697. These observation results show that the axisymmetric flow is maintained at the Reynolds number up to one thousand and few hundreds.

Figure 7 shows the experimental observations of the flows from the side views. The inner and the outer cylinders are on the left and the right sides, respectively. In the figure, the region near the

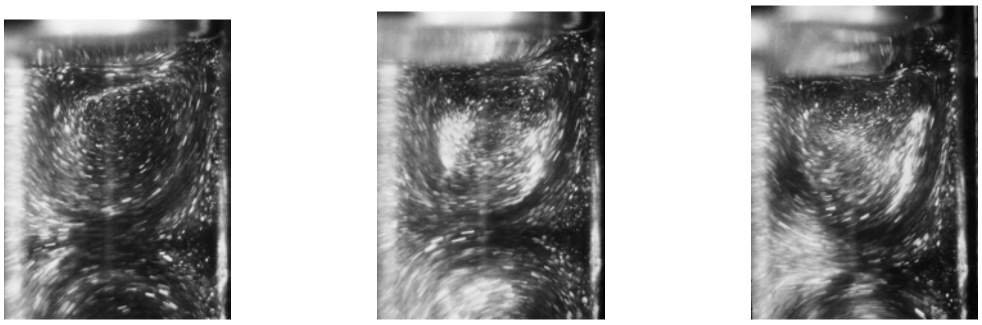

Fig. 7. Experimental observations of free surface flows in side views. The upper most vortices of the normal five-cell mode flows are shown. Γ = 5.7.

free surface in the normal five-cell mode flow is enlarged, where the upper most vortex rotating in the clockwise direction and the half of the neighboring lower vortex appear. At larger Reynolds number, the vortex at the top is deformed.

4. Conclusion

Toroidal vortex flows in an asymmetric Taylor-Couette system with a free surface on the top are investigated.

Bifurcation locus between the normal one-cell mode and the normal three-cell mode and the locus between the normal three-cell mode and the normal five-cell mode are determined in the space of the aspect ratio and the Reynolds number. The critical Reynolds number of the mode exchanges decreases with the aspect ratio.

The variances of the time-dependent properties grow when the Reynolds number reaches at its critical values of mode exchanges. This shows that the mode exchanges accompany with the increase in the time-dependent behavior of the global flows.

References

Baier, G. and Graham, M. D., Two-fluid Taylor-Couette flow: experiments and linear theory for immiscible liquids between corotating cylinders, Phys. Fluids, 10-12 (1998), 3045-3055.

Batchelor, G. K., An introduction to fluid dynamics, Chap. 1, (1967), Cambridge Univ. Press.

Bellon, L., Fourten, L., Minassian, V. T. and Rabaud, M., Wave-number selection and parity-breaking bifurcation in directional viscous fingering, Phys. Rev. E, 58-1 (1998), 565-574.

Benjamin, T. B., Bifurcation phenomena in steady flows of a viscous fluid II Experiments, Proc. Roy. Soc. Lond., Ser. A., 359 (1978), 27-43.

Di Prima, R. C. and Swinney, H. L., Instabilities and transition in flow between concentric rotating cylinders, Hydrodynamics instabilities and the transition to turbulence, eds. Swinney H. L. and Gollub J. P., Chap. 6, (1981), Springer.

Fraňa, K., Stiller, J. and Grudmann, R., Taylor-Görtler vortices in the flow driven by a rotating magnetic field in a Cylindrical Container, J. of Visualization, 8-4 (2005), 323-330.

Gelfgat, A. Y., Yarin, A. L., Bar-Yoseph, P. Z., Graham, M. D. and Bai, G., Numerical modeling of two-fluid Taylor-Couette flow with deformable capillary liquid-liquid interface, Phys. Fluids, 16-11 (2004), 4066-4074.

Hantao, J., et al., Hydrodynamic turbulence cannot transport angular momentum effectively in astrophysical disks, Nature, 444-16 (2006), 343-346.

Linek, M. and Ahlers, G., Boundary limitation of wave numbers in Taylor-vortex flow, Phys. Rev. E., 58-3 (1998), 3168-3174.

Michalland, S., Rabaud, M. and Couder, Y., Transition to chaos by spatio-temporal intermittency in directional viscous fingering, Europhysics Lett., 22-1 (1993), 17-22.

Nakamura, I. and Toya, Y., Existence of extra vortex and twin vortex of anomalous mode in Taylor vortex flow with a small aspect ratio, Acta Mechanica, 117 (1996), 33-46.

Nakamura, I., Toya, Y., Yamashita, S. and Ueki, Y., An experiment on a Taylor vortex flow in a gap with a small aspect ratio (instability of Taylor vortex flows), JSME International Journal, Ser. II, 32-3 (1989), 388-394.

Tagg, R., The Couette-Taylor problem, Nonlinear Science Today, 4-3 (1994), 2-25.

Toya, Y., Nakamura, I., Yamashita, S. and Ueki, Y., An experiment on a Taylor vortex flow in a gap with a small aspect ratio -- Bifurcation of flows in an asymmetric system --, Acta Mechanica, 102 (1994), 137-148.

Watanabe, T., Furukawa, H. and Nakamura, I., Nonlinear development of flow patterns in an annulus with decelerating inner cylinder, Phys. Fluids, 14-1 (2002), 333-341.

Author Profile

Takashi Watanabe: He received his Ph.D degree (Eng.) from Nagoya University in 1986. He now works as a professor at the EcoTopia Science Institute, Nagoya University. His current research interests are the computational fluid dynamics of rotating flows and the human-computer interfaces. He is a member of the Japan Society of Mechanical Engineers, the Japan Society of Fluid Mechanics and the Japanese Society for Artificial Intelligence.

Hiroyuki Furukawa: He received the BE degree in mechanical engineering from Nagoya University (1997) and the MA degree and Ph.D degree in human informatics from Nagoya University (1999). He now works as an associate professor at Meijo University. His researches include flow transient, flow visualization and non-linear dynamics.

Yorinobu Toya: He received Ph.D degree (Eng.) from Nagoya University in 1994. He works as a professor at Mechanical Engineering in Nagano National College of Technology. His current researches are the experimental and numerical studies for the circulating flows between rotating cylinders.